Cellular/Molecular

Charged Residues in the α_1 and β_2 Pre-M1 Regions Involved in $GABA_A$ Receptor Activation

Jose Mercado and Cynthia Czajkowski
Department of Physiology and Neuroscience Training Program, University of Wisconsin–Madison, Madison, Wisconsin 53706

For Cys-loop ligand-gated ion channels (LGIC), the protein movements that couple neurotransmitter binding to channel gating are not well known. The pre-M1 region, which links the extracellular agonist-binding domain to the channel-containing transmembrane domain, is in an ideal position to transduce binding site movements to gating movements. A cluster of cationic residues in this region is observed in all LGIC subunits, and in particular, an arginine residue is absolutely conserved. We mutated charged pre-M1 residues in the $GABA_A$ receptor α_1 (K219, R220, K221) and β_2 (K213, K215, R216) subunits to cysteine and expressed the mutant subunits with wild-type β_2 or α_1 in *Xenopus* oocytes. Cysteine substitution of β_2R216 abolished channel gating by GABA without altering the binding of the GABA agonist [^{3}H]muscimol, indicating that this residue plays a key role in coupling GABA binding to gating. Tethering thiol-reactive methanethiosulfonate (MTS) reagents onto α_1K219C, β_2K213C, and β_2K215C increased maximal GABA-activated currents, suggesting that structural perturbations of the pre-M1 regions affect channel gating. GABA altered the rates of sulfhydryl modification of α_1K219C, β_2K213C, and β_2K215C, indicating that the pre-M1 regions move in response to channel activation. A positively charged MTS reagent modified β_2K213C and β_2K215C significantly faster than a negatively charged reagent, and GABA activation eliminated modification of β_2K215C by the negatively charged reagent. Overall, the data indicate that the pre-M1 region is part of the structural machinery coupling GABA binding to gating and that the transduction of binding site movements to channel movements is mediated, in part, by electrostatic interactions.

Key words: **GABA; $GABA_A$ receptor; pre-M1 region; substituted cysteine accessibility method; electrostatic interactions; allosteric protein; ligand-gated ion channel**

Introduction

For ligand-gated ion channels (LGIC), neurotransmitter binding triggers a series of conformational movements that ultimately lead to channel opening. Because the neurotransmitter binding site resides on the extracellular surface of the protein and the channel gate is located in the transmembrane domain (TMD), the local changes that occur at the binding site when neurotransmitter binds must be propagated to distant parts of the receptor protein. Although much is known about the structure of the Cys-loop superfamily of LGICs from the recent 4 Å resolution model of the *Torpedo* nicotinic acetylcholine receptor (nAChR) (Unwin, 2005) and the crystallographic structure of the related acetylcholine binding protein (AChBP) (Brejc et al., 2001; Celie et al., 2004), these structures alone cannot describe the protein dynamics involved in coupling neurotransmitter binding to channel gating.

The N-terminal region of the first transmembrane domain (pre-M1), a region that structurally links the extracellular ligand binding domain (LBD) to the transmembrane channel domain, is in an ideal position to transduce binding site movements in the extracellular domain to gating movements in the membrane domains. It physically links β-strand 10, which forms part of loop C of the binding site, to the first transmembrane α-helix M1. In addition, a cluster of cationic residues in this region is observed in all LGIC subunits, and in particular, the arginine at $\beta_2$216 of the $GABA_A$ receptor ($GABA_AR$) and aligned positions is absolutely conserved (see Fig. 1), suggesting that charge interactions may play a role in coupling ligand binding to channel gating. Here, we used the substituted cysteine accessibility method to examine the electrostatic environment and dynamics of the pre-M1 region of the $GABA_A$ receptor during channel activation.

Charged amino acid residues in the pre-M1 regions of the α_1 and β_2 subunits of the $GABA_A$ receptor were individually mutated to cysteine. The rates these cysteines were modified by sulfhydryl-specific methanethiosulfonate (MTS) reagents were measured in unliganded (resting) and GABA-bound receptor states (open/desensitized) to determine whether structural movements occur in the pre-M1 region during channel activation. In addition, we used MTS reagents of different charge to monitor the electrostatic environment near the pre-M1 region.

We demonstrate that both the α_1 and β_2 pre-M1 regions undergo structural rearrangements during channel activation, as expected if this region is an important transduction element cou-

Received Oct. 24, 2005; revised Jan. 5, 2006; accepted Jan. 6, 2006.

This work was supported in part by the Diversity Program in Neuroscience of the American Psychological Association (J.M.) and by National Institute of Neurological Disorders and Stroke–National Institutes of Health Grant NS34727 (C.C.). We thank Dr. Ken Satyshur for assistance with construction of the structural model and Dr. Andrew Boileau for helpful discussion. We also thank Whitney Pafford and Srinivasan Venkatachalan for treating the oocytes.

Correspondence should be addressed to Dr. Cynthia Czajkowski, University of Wisconsin–Madison, 601 Science Drive, Madison, WI 53711. E-mail: czajkowski@physiology.wisc.edu.

DOI:10.1523/JNEUROSCI.4555-05.2006

 0270-6474/06/262031-10$15.00/0

pling binding to gating. Moreover, we provide evidence that mutation of the conserved arginine residue at position 216 in the β_2 subunit to cysteine uncouples agonist binding from gating. Oocytes expressing $\alpha_1\beta_2$R216C receptors had no functional response to GABA but specifically bound the GABA agonist [^{3}H]muscimol to similar levels as wild-type receptors. Differences in the accessibility and the functional effects of oppositely charged MTS compounds suggest that unliganded and liganded receptor state stabilization is mediated, in part, by electrostatic forces. Overall, the data indicate that the pre-M1 region is part of the structural machinery linking binding site movements to channel gating movements.

Materials and Methods

Mutagenesis. Rat cDNAs encoding α_1 and β_2 $GABA_A$ receptor subunits were used for all molecular cloning and functional studies. Cysteine mutants were made using either the QuickChange site-directed mutagenesis kit (Stratagene, La Jolla, CA) or by recombinant PCR, as described previously (Boileau et al., 1999). Mutagenic oligonucleotides were synthesized to introduce the desired mutation, and a silent restriction site was used to screen for the desired mutations. All mutant cDNA was verified by double-stranded cDNA sequencing to confirm that the desired point mutations was present and that the cDNA was free of additional mutations.

Expression in Xenopus laevis *oocytes.* Oocytes were prepared as described previously (Boileau et al., 1998). Capped cRNAs encoding the α_1, β_2, α_1K219C, α_1R220C, α_1K221C, β_2K213C, β_2K215C, and β_2R216C subunits in the vector pGH19 (Liman et al., 1992; Robertson et al., 1996) were transcribed *in vitro* using the mMessage mMachine T7 kit (Ambion, Austin, TX). Single oocytes were injected within 24 h with 27 nl of cRNA (10 ng/μl per subunit) in a ratio of 1:1. Oocytes were incubated at 18°C in ND96 (in mM: 96 NaCl, 2 KCl, 1 $MgCl_2$, 1.8 $CaCl_2$, and 5 HEPES, pH 7.2), supplemented with 100 μg/ml gentamycin and 100 μg/ml BSA, for 2–14 d before use.

Two-electrode voltage clamp. Oocytes were perfused continuously at a rate of 5 ml/min with ND96 while being held under two-electrode voltage clamp at −80 mV. The bath volume was ~200 μl. Stock solutions of GABA (Sigma, St. Louis, MO), muscimol (Sigma), and pentobarbital (Research Biochemicals, Natick, MA) were prepared fresh in ND96. Borosilicate electrodes (Warner Instruments, Hamden, CT) were filled with 3 M KCl and had resistances between 0.7 and 2 MΩ. Electrophysiological data were acquired with a GeneClamp 500 (Molecular Devices, Sunnyvale, CA) interfaced to a computer with an ITC16 analog-to-digital device (Instrutech, Great Neck, NY) and recorded using the Whole Cell program, version 3.2.9 (kindly provided by J. Demspter, University of Strathclyde, Glasgow, UK).

Concentration–response analysis. Concentration–response experiments were performed as described previously (Boileau and Czajkowski, 1999). In brief, GABA concentration–responses were scaled to a low, nondesensitizing concentration of GABA (EC_2 to EC_{10}) applied just before the test concentration to correct for any slow drift in I_{GABA} responsiveness over the course of the experiment. Currents elicited by each test concentration were normalized to the corresponding low concentration current before curve fitting. GraphPad (San Diego, CA) Prism 4 software was used for data analysis and fitting. Concentration–response data were fit to the following equation: $I = I_{max}/(1 + (EC_{50}/[A])^n)$, where I is the peak response to a given concentration of GABA, I_{max} is the maximum amplitude of current, $[A]$ is the agonist concentration, and n is the Hill coefficient.

Modification of introduced cysteine residues by MTS reagents. Three derivatives of methanethiosulfonate (CH_3SO_2X) were used to covalently modify the introduced cysteines: MTS-N-biotinylaminoethyl [X = SCH_2CH_2NH-biotin (MTSEA-biotin)], MTS-ethyltrimethylammonium [$X = SCH_2CH_2N(CH_3)_3^+$ ($MTSET^+$)], and MTS-ethylsulfonate [$X = SCH_2CH_2SO_3^-$ ($MTSES^-$)] (Biotium, Hayward, CA). Stocks solutions (100 mM) were made in DMSO for all MTS reagents, aliquoted into microcentrifuge tubes, and rapidly frozen on ice before storage at −20°C. For each application of MTS reagent, a new aliquot was thawed, diluted in ND96 to the working concentration, and used immediately to avoid hydrolysis of the MTS compound. The final DMSO concentrations were ≤2%. These solvent concentrations did not affect $GABA_A$ receptor functional responses.

MTS modifications of the engineered cysteines were assayed by measuring changes in GABA-evoked current (I_{GABA}). The effects of MTSEA-biotin, $MTSET^+$, and $MTSES^-$ were studied using the following protocol: GABA (EC_{40-60}) current responses (10–30 s) were measured from oocytes expressing wild-type ($\alpha_1\beta_2$) or mutant receptors and stabilized. Stability was defined as <5% variance of peak current responses to GABA on two consecutive applications. After stabilization, the MTS reagent (2 mM) was bath applied for 2 min, followed by a 5–7 min wash, and then I_{GABA} was measured at the same concentration as before the MTS treatment. The effect of the MTS application was calculated as follows: $[((I_{after}/I_{initial}) - 1) \times 100]$, where I_{after} is the peak GABA current elicited after the MTS application and $I_{initial}$ is the peak current before MTS. Maximal I_{GABA} was also measured, before and after MTS application using 10 and 300 mM GABA. In these cases, the time interval between GABA applications was 9–12 min to allow complete recovery from desensitization.

Rate of MTS modification. The rates at which the various MTS reagents modified the engineered cysteines were determined by measuring the effect of sequential applications of low concentrations of MTS reagents on I_{GABA}, as described previously (Holden and Czajkowski, 2002). The protocol is described as follows: EC_{40-60} GABA was applied for 10 s every 3–5 min until I_{GABA} stabilized (<3% variance). After a 40 s ND96 washout, MTS reagents were applied for 5–20 s, and the cell was then washed for an additional 2.5–4.5 min. The procedure was repeated until I_{GABA} no longer changed, indicating that the reaction had proceeded to apparent completion. Concentration of MTS reagent and time of application varied as follows: α_1K219C: MTSEA-biotin, 10 μM, 20 s; α_1K221C: MTSEA-biotin, 10 μM, 20 s; $MTSES^-$, 300 μM, 20 s; β_2K213C: $MTSET^+$, 30 μM, 20 s; $MTSES^-$, 500 μM, 20 s; β_2K215C: $MTSET^+$, 30 μM, 20 s; $MTSES^-$, 300 μM, 20 s. The effects of GABA on the rate of MTS modification were measured by coapplying GABA (EC_{80-90}) with the MTS reagent. For these experiments, I_{GABA} was stabilized as follows: EC_{40-60} GABA was applied for 10 s, washed for 40 s; EC_{80-90} GABA was applied for 5–20 s, washed for 2.5–5 min. The procedure was repeated until I_{GABA} from EC_{40-60} GABA was within <3% of the previous I_{GABA} peak. This ensured complete washout of the drug and that any alteration in the current amplitudes after MTS treatment was the result of MTS modification. Concentrations of MTS reagents and times of applications in the presence of GABA (EC_{80-90}) were as follows: α_1K219C: MTSEA-biotin, 30 μM, 20 s; α_1K221C: MTSEA-biotin, 10 μM, 20 s; β_2K213C: $MTSET^+$, 30 or 60 μM, 10 s; β_2K215C: $MTSET^+$, 30 μM, 10 s.

For all rate experiments, the decrease or increase in GABA-induced current was plotted versus cumulative time of MTS exposure. Peak current at each time point was normalized to the initial peak current ($t = 0$) and fit to a single exponential function using GraphPad Prism software. A pseudo-first-order rate constant (k_1) was determined, and a second-order rate constant (k_2) was calculated by dividing k_1 by the concentration of the MTS reagent used (Pascual and Karlin, 1998).

[^{3}H]Muscimol single oocyte binding. For binding experiments, the concentration of cRNA injected was 5.4 ng per subunit. Intact oocytes were washed twice with PBS (in mM: 137.93 NaCl, 2.67 KCl, 1.5 KH_2PO_4, and 8 $Na_2HPO_4 \cdot 7H_2O$, pH 7.1). To measure total [^{3}H]muscimol binding sites, intact oocytes (8 or 10) were incubated on ice in PBS with 150 nM [^{3}H]muscimol (15.7 Ci/mmol; DuPont NEN, Boston, MA) in triplicate (final volume, 0.5 ml). Nonspecific binding was determined in the presence of 100 μM muscimol. After a 1 h incubation on ice, the samples were vacuum filtered over GF/B glass microfiber filters (Whatman, Clifton, NJ) using a Hoefer Scientific (San Francisco, CA) vacuum box (model FH224) and washed four times with 5 ml of ice-cold PBS. The filters and oocytes were mixed thoroughly with 4 ml of scintillation fluid, and the radioactivity (in counts per minute) was determined. Specific binding was defined as the amount of [^{3}H]muscimol bound in the absence of displacing ligand (total) minus the amount bound in the presence of 100 μM muscimol (nonspecific).

Statistical analysis. Log (EC_{50}) values, changes in GABA EC_{50} and

maximal response after MTS modification, and second-order (k_2) rates were analyzed generally using a one-way ANOVA, followed by a *post hoc* Dunnett's test to determine the level of significance between wild-type and mutant receptors. Comparison of the second-order (k_2) rates of covalent modification of β_2K213C and β_2K215C in the absence and presence of GABA were performed using Student's one-tailed paired *t* test. Alterations in GABA EC_{50} resulting from MTS treatment were analyzed using Student's two-tailed paired *t* test.

Structural modeling. A model of the extracellular LBD of the $GABA_A$ receptor was built based on the structure of the AChBP (Brejc et al., 2001). The crystal structure of the AChBP was downloaded from Research Collaboratory for Structural Bioinformatics Protein Data Bank (code 1I9B) and loaded into Swiss Protein Bank Viewer (SPDBV; http://www.expasy.org/spdbv/). The rat α_1 mature protein sequence from Thr^{12} to Ile^{227}, the β_2 protein sequence from Ser^{10} to Leu^{218}, and the γ_2 protein sequence from Gly^{25} to Arg^{231} were aligned with the AChBP primary amino acid sequence as depicted by Cromer et al. (2002) and threaded onto the AChBP tertiary structure using the "Interactive Magic Fit" function of SPDBV. The threaded subunits were imported into SYBYL (Tripos, St. Louis, MO), where energy minimization was performed. SYBYL minimizations terminate when the number of iterations is reached or if the gradient change reaches 0.05 kcal/Å·mol. The first 100 iterations were performed using Simplex minimization (Press et al., 1998) followed by 1000 iterations using the Powell conjugate gradient method (Powell, 1977). A $GABA_A$ receptor LBD (β:α:β:α:γ viewed counterclockwise from the synaptic cleft) was assembled by overlaying the monomeric subunits on the AChBP scaffold, and the resulting structure was imported into SYBYL and energy minimized. Neither water nor entropy factors were included during the minimizations. After the global energy minimization, Ramachandran plots, χ plots, side-chain positions, and *cis* and *trans* bonds were all examined. The program PROCHECK (Laskowski et al., 1996) was run to examine structural features against the established database of protein parameters, most importantly the ϕ/ψ torsions and side-chain conformations. Problems in the structure that were revealed by these evaluations were fixed manually, and energy minimizations were run again as needed. Regions with insertions were modeled by fitting structures from a loop database. Because the sequence identity of the AChBP and the $GABA_A$ receptor LBD is only 18%, caution must be used in interpreting the absolute positions of individual side-chain residues in the model.

The structure of the nAChR transmembrane domain at 4 Å resolution solved by Miyazawa et al. (2003) (PDB 1OED) was used to model the pore-containing TMDs of the $GABA_A$ receptor. The $GABA_A$ receptor TMD sequences were aligned with the nAChR TMD sequences and the amino acids from the α_1, β_2, and γ_2 subunits of the $GABA_AR$ were substituted for residues in the γ/δ, α, and β nAChR subunits, respectively. The TMD of each subunit was built and energy minimized individually using the Tripos force field program in SYBYL. A $GABA_A$ receptor TMD pentamer was assembled by overlaying the monomeric subunits on the nAChR scaffold, and the resulting structure was imported into SYBYL and energy minimized as described above.

A model of the entire $GABA_A$ receptor (LBD plus TMD) was built by physically docking the LBD model with the TMD model using the fivefold axes as a docking guide. The domains were rotated so that their relative positions to one another were consistent with published experimental data. The TMD N-terminal and the LBD C-terminal residues were joined and energy minimized while fixing the rest of the molecule. This was followed by an energy minimization of the entire structure in three stages. The first stage used the Simplex method for 20 cycles before switching to the Tripos force field for 1000 iterations. Finally, the third stage again used the Tripos force field with >1000 cycles, or a convergence of <0.05 kcal/Å·mol. After the global energy minimization, Ramachandran plots, χ plots, side-chain positions, and *cis* and *trans* bonds were all examined. The program PROCHECK (Laskowski et al., 1996) was run to examine structural features against the established database of protein parameters, most importantly the ϕ/ψ torsions and side-chain conformations. Problems in the structure that were revealed by these evaluations were fixed manually and energy minimizations were run again as needed. Although the resulting model is reasonable, the packing of the loops at the interface of the LBD and TMD as well as the positions of residue side-chains need to be interpreted with care.

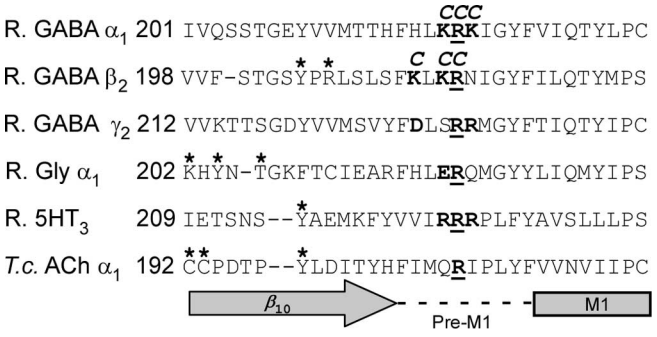

Figure 1. Aligned amino acid sequences of the pre-M1 and adjacent regions of the rat (R) $GABA_A$ receptor α_1, β_2, and γ_2 subunits, rat glycine receptor α_1 subunit, rat serotonin type-3 receptor subunit, and the *T. californica* (*T.c.*) nicotinic acetylcholine receptor α_1 subunit. Aligning $GABA_A$ receptor subunit sequences with other LGIC subunits reveals a cluster of charged residues in the pre-M1 region. Cationic and anionic residues in the pre-M1 regions are in boldface. The $GABA_A$ receptor arginine residues at $\alpha_1$220 and $\beta_2$216 are conserved in all LGIC subunits (underlined). Residues mutated to cysteine are marked with a "C" above the residue. Residues located in the GABA binding site, β_2Y205 and β_2R207 (Amin and Weiss, 1993; Wagner and Czajkowski, 2001), and the binding sites of other LGICs (Kao et al., 1984; Mishina et al., 1985; Dennis et al., 1988; Ruiz-Gomez et al., 1990; Galzi et al., 1991a,b; Vandenberg et al., 1992a,b; Rajendra et al., 1995) are marked with an asterisk. Elements of secondary structure are indicated below the sequences by the arrow (β-strand 10) and rectangle (α helix, M1 transmembrane region).

Results

Functional characterization of pre-M1 mutant receptors

Three charged residues in the α_1 subunit (K219, R220, and K221) and in the β_2 subunit (K213, K215, and R216) were mutated to cysteine in the pre-M1 region (Fig. 1). Oocytes were injected with each of the mutant subunits, wild-type β_2, or α_1 and were assayed for GABA responsiveness using two-electrode voltage clamp. GABA elicited currents (I_{GABA}) from oocytes expressing α_1K219Cβ_2, α_1K221Cβ_2, $\alpha_1\beta_2$K213C, and $\alpha_1\beta_2$K215C receptors, indicating that these cysteine substitutions were tolerated and yielded functional receptors. The GABA EC_{50} and Hill coefficient values were not significantly different from wild-type values (EC_{50} = 6.9 ± 0.7 μM; n_H = 1.0 ± 0.1) (Fig. 2, Table 1). Oocytes expressing α_1K219Cβ_2, α_1K221Cβ_2, $\alpha_1\beta_2$K213C, and $\alpha_1\beta_2$K215C receptors elicited maximal macroscopic currents similar to wild-type receptors (2130 ± 885 nA; n = 8).

Neither GABA (1 mM) nor pentobarbital (1 mM) elicited current responses from oocytes expressing α_1R220C plus β_2 or α_1 plus β_2R216C combinations of subunits (Fig. 3*A*), suggesting that cysteine substitutions at these positions affected receptor assembly/surface expression or that surface mutant receptors were expressed but were unresponsive to GABA and pentobarbital. To help distinguish between these possibilities, we measured the binding of [^{3}H]muscimol to surface receptor protein using an intact oocyte binding assay. Intact oocytes expressing $\alpha_1\beta_2$R216C receptors specifically bound similar amounts of [^{3}H]muscimol (4 ± 0.9 fmols per oocyte; n = 3) as wild-type $\alpha_1\beta_2$ receptors (3 ± 0.4 fmols per oocyte; n = 3) (Fig. 3*B*), suggesting that the β_2R216C mutation does not appear to affect receptor expression or agonist binding but uncouples ligand binding from channel gating. Oocytes expressing α_1R220Cβ_2 receptors did not bind [^{3}H]muscimol and were not gated by GABA or pentobarbital (Fig. 3), suggesting that cysteine substitution of α_1R220 was not tolerated.

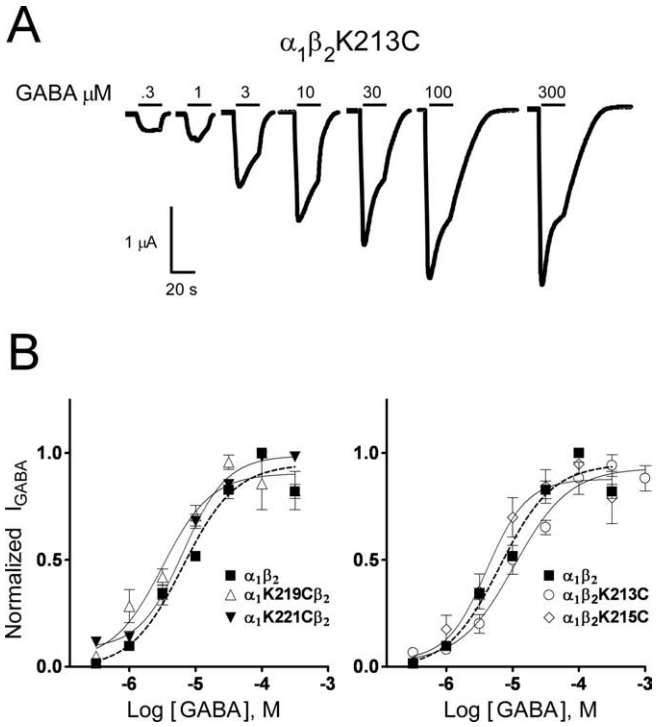

Figure 2. GABA concentration–response curves of wild-type $\alpha_1\beta_2$ and mutant GABA$_A$ receptors. ***A***, Representative current responses from an oocyte expressing $\alpha_1\beta_2$K213C receptors elicited by increasing concentrations of GABA (micromolar). ***B***, GABA concentration–response curves from oocytes expressing $\alpha_1\beta_2$ (■; dashed line), α_1K219Cβ_2 (△), α_1K221Cβ_2 (▼), $\alpha_1\beta_2$K213C (○), and $\alpha_1\beta_2$K215C (◇) receptors. Data points represent the mean ± SEM from three to four independent experiments. Data were fit by nonlinear regression analysis as described in Materials and Methods. GABA EC_{50} and n_H values are reported in Table 1.

Table 1. GABA EC_{50} and Hill coefficient values of wild-type and mutant receptors

Receptor	EC_{50} (μM)	n_H	*n*
$\alpha_1\beta_2$	6.9 ± 0.7	1.0 ± 0.1	4
α_1K219Cβ_2	2.5 ± 1.6	1.6 ± 0.4	4
α_1R220Cβ_2	NM	NM	
α_1K221Cβ_2	7.9 ± 0.8	1.7 ± 0.1	3
$\alpha_1\beta_2$K213C	13.5 ± 3.5	1.4 ± 0.4	3
$\alpha_1\beta_2$K215C	4.3 ± 3.8	1.5 ± 0.4	4
$\alpha_1\beta_2$R216C	NM	NM	

EC_{50} and Hill coefficient values are expressed as mean ± SEM. NM, Not measurable as a result of no observable GABA-mediated current responses.

MTS effects on substituted cysteines

To explore the physicochemical environment of the pre-M1 region, we examined the ability of MTS reagents that differ in size and charge to modify wild-type, α_1K219Cβ_2, α_1K221Cβ_2, $\alpha_1\beta_2$K213C, and $\alpha_1\beta_2$K215C receptors. The MTS reagents (Fig. 4*A*) used were: MTSEA-biotin, which covalently adds a neutral biotinylaminoethyl group (12 Å long); $MTSET^+$, which adds a positively charged ethyl-trimethylammonium group (4.5 Å long); and $MTSES^-$, which adds a negatively charged ethylsulfonate group (4.8 Å long). Application of 2 mM MTSEA-biotin, $MTSET^+$, and $MTSES^-$ for 2 min to wild-type receptors had no effect on I_{GABA} (EC_{50} concentration), indicating that any effects observed in the mutant receptors were caused by covalent modification of the introduced cysteines (Fig. 4*B*). MTSEA-biotin modification of α_1K219C, β_2K213C, and β_2K215C increased I_{GABA} by 34 ± 2, 34 ± 9, and 34 ± 2% ($n \geq 3$), respectively, and decreased I_{GABA} by 60 ± 4% ($n = 9$) in α_1K221C-containing receptors (Fig. 4*B*).

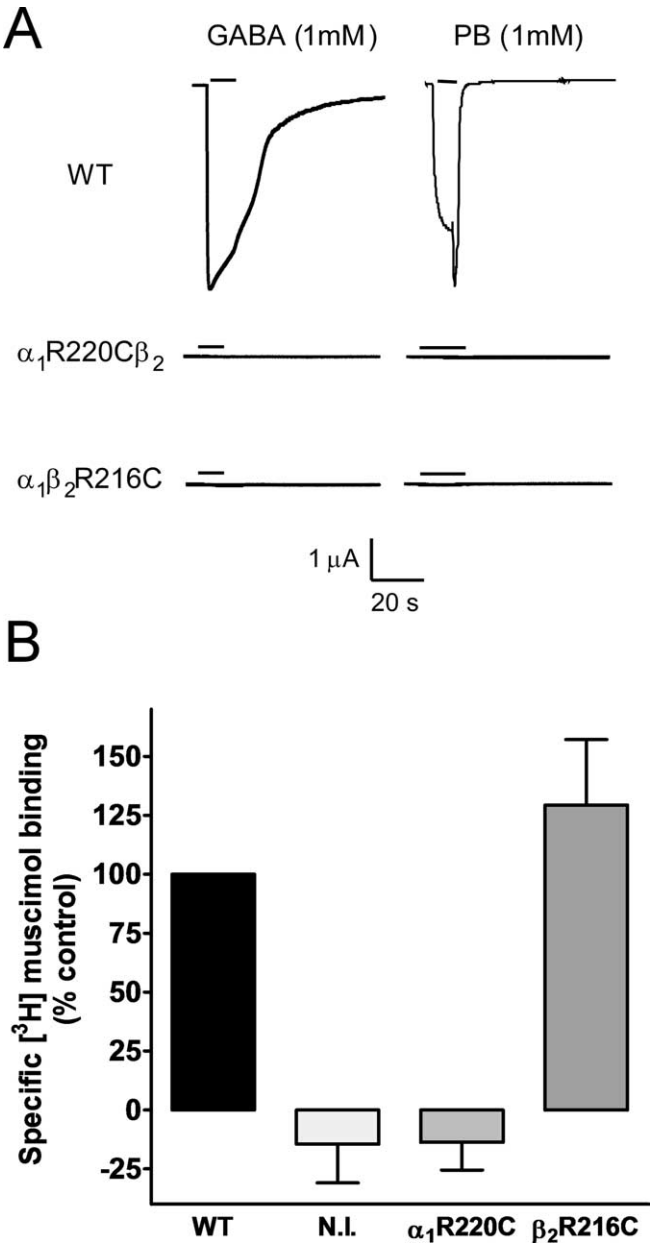

Figure 3. Expression of $\alpha_1\beta_2$, α_1R220Cβ_2, and $\alpha_1\beta_2$R216C GABA$_A$ receptors. ***A***, Representative GABA- (1 mM) and pentobarbital- (PB; 1 mM) mediated current responses from oocytes injected with $\alpha_1\beta_2$ [wild type (WT)], α_1R220C plus β_2, and α_1 plus β_2R216C cRNA. Neither GABA nor pentobarbital elicited current responses from oocytes expressing α_1R220C or β_2R216C subunits. ***B***, Specific [^{3}H]muscimol binding was measured in intact oocytes expressing WT and mutant subunits as described in Materials and Methods. Data were normalized to the specific [^{3}H]muscimol binding measured for WT receptors. Noninjected oocytes (N.I.) and oocytes injected with α_1R220Cβ_2 subunits did not specifically bind [^{3}H]muscimol. Oocytes expressing $\alpha_1\beta_2$R216C receptors specifically bound similar amounts (129 ± 28%) of [^{3}H]muscimol as oocytes expressing WT receptors. Error bars represent the mean ± SEM from three independent experiments.

Derivatization of β_2K213C and β_2K215C with $MTSES^-$ increased I_{GABA} by 47 ± 5 and 48 ± 7%, respectively, whereas $MTSET^+$ increased I_{GABA} by 95 ± 8 and 53 ± 4%, respectively ($n \geq 8$) (Fig. 4*B*). In contrast, modification of α_1K219Cβ_2 and α_1K221Cβ_2 by $MTSES^-$ and $MTSET^+$ differentially affected I_{GABA} (Fig. 4*B*). Tethering a negative charge ($MTSES^-$) on α_1K221Cβ_2 enhanced I_{GABA} (98 ± 14%; $n = 4$), whereas treatment with the positively charged $MTSET^+$ had no effect on I_{GABA}

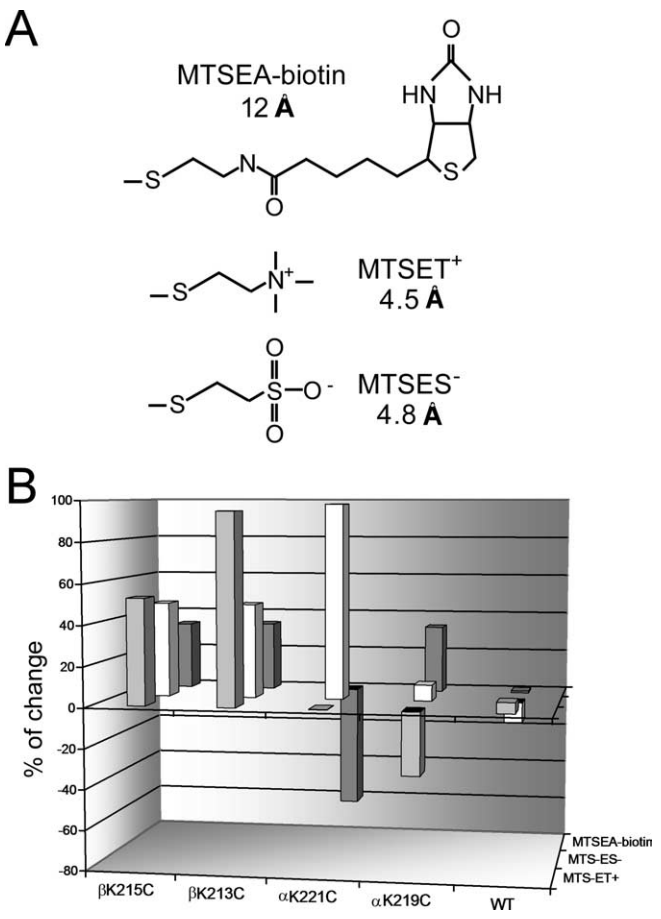

Figure 4. Effects of MTS reagents on wild-type and mutant $GABA_A$ receptors. ***A***, Structures of MTS reagents represent the portions of the reagents that covalently modify an introduced cysteine. Lengths were measured after energy minimization (<0.5 kcal/Å; ChemSketch; Advanced Chemistry Development, Toronto, Ontario, Canada). ***B***, Effects of a 2 min application of 2 mM MTSEA-biotin, $MTSET^+$, or $MTSES^-$ on wild-type (WT) and mutant receptors. The percentage change in I_{GABA} after MTS treatment is defined as follows: $[((I_{after}/I_{initial}) - 1) \times 100]$. Negative values represent an inhibition of I_{GABA} after MTS reaction, whereas positive values represent an increase in I_{GABA}. Data represent the mean from at least four independent experiments. All of the effects observed on the mutated receptors after MTS modification, except for $\alpha_1K221C\beta_2$ plus $MTSET^+$ and $\alpha_1K219C\beta_2$ plus $MTSES^-$, were statistically significant from wild type ($p < 0.01$).

(Fig. 4*B*). To determine whether $MTSET^+$ reacted with α_1K221C, we first applied $MTSET^+$ and then $MTSES^-$ to the same oocyte. The ability of $MTSES^-$ to potentiate subsequent GABA currents was eliminated by pretreatment with $MTSET^+$ (data not shown), indicating that $MTSET^+$ covalently modified α_1K221C, but modification had no effect in our functional assay (silent reaction). In contrast to the effects seen on α_1K221C, tethering $MTSET^+$ on α_1K219C decreased I_{GABA} (31 ± 7%; $n = 3$), whereas modification with $MTSES^-$ had no effect (silent reaction). The different functional effects measured after $MTSES^-$ and $MTSET^+$ modification of α_1K219C and α_1K221C are likely caused by differences in the local electrostatic environments near these residues rather than steric effects, because $MTSET^+$ and $MTSES^-$ are similar in size (Fig. 4*A*) and have a common reaction mechanism.

As described above, cysteine substitution of β_2R216 abolished channel gating by GABA without altering [^{3}H]muscimol binding (Fig. 3). To determine whether restoring the positive charge at this position would restore channel gating by GABA, we measured whether GABA would elicit current responses from $\alpha_1\beta_2$R216 receptors after $MTSET^+$ exposure. Application of 2 mM $MTSET^+$ for 2 min to $\alpha_1\beta_2$R216C receptors had no effect on I_{GABA} (data not shown), suggesting that tethering the positively charged ethyl-trimethylammonium group from $MTSET^+$ was insufficient to restore $GABA_AR$ current responses or that the introduced cysteine was not modified.

MTS effects on maximal GABA current

An increase or decrease in I_{GABA} after MTS application can be attributed to a change in GABA apparent affinity (EC_{50}) and/or a change in maximal GABA response (I_{max}). To test whether MTS modification altered GABA I_{max}, we measured current responses elicited from GABA EC_{50} concentrations (I_{EC50}) and saturating concentrations of GABA (10 and 300 mM; I_{max}) before and after MTS application (Fig. 5). MTSEA-biotin was used for the α_1 mutants (α_1K219Cβ_2, α_1K221Cβ_2) and $MTSET^+$ for the β_2 mutants ($\alpha_1\beta_2$K213C, $\alpha_1\beta_2$K215C). Application of 2 mM MTSEA-biotin or $MTSET^+$ for 2 min to wild-type receptors did not affect I_{EC50} *or* I_{max} (Fig. 5). MTS modification significantly increased I_{max} for α_1K219Cβ_2 (34 ± 3%), $\alpha_1\beta_2$K213C (37 ± 7%), and $\alpha_1\beta_2$K215C (43 ± 5%) receptors ($n \geq 4$; $p < 0.01$), suggesting that tethering thiol-reactive groups at these positions caused changes in channel gating or conductance. MTSEA-biotin significantly reduced I_{max} by 55 ± 3% (Fig. 5) for α_1K221Cβ_2 receptors ($n = 7$; $p < 0.01$). Although the results are consistent with a decrease in channel gating at this position, we cannot rule out the possibilities that a subset of receptor channels might be blocked by the MTS compound or that modification causes an enormous increase in the unbinding of GABA, which could contribute to the decrease in I_{max} measured.

To estimate whether the MTS modifications were also altering GABA apparent affinity, we calculated the I_{EC50}/I_{max} ratio of current responses (R) after MTS treatment for each mutant receptor. Assuming that MTS modification did not significantly alter the Hill coefficients, we would expect a ratio of 0.5 if the MTS modification had no effect on GABA EC_{50}, a ratio >0.5 if GABA EC_{50} decreased, and a ratio <0.5 if GABA EC_{50} increased. The I_{EC50}/I_{max} ratio did not alter significantly for α_1K219Cβ_2 (R_{before}, 0.44 ± 0.02; R_{after}, 0.43 ± 0.02) and $\alpha_1\beta_2$K215C receptors (R_{before}, 0.47 ± 0.02; R_{after}, 0.50 ± 0.03) but increased significantly for $\alpha_1\beta_2$K213C receptors (R_{before}, 0.47 ± 0.04; R_{after}, 0.67 ± 0.05 μM) and decreased significantly at α_1K221Cβ_2 receptors (R_{before}, 0.46 ± 0.02; R_{after}, 0.29 ± 0.05 μM) ($n \geq 3$; $p < 0.05$), suggesting that covalent modification of α_1K221C and β_2K213C altered GABA apparent affinity. No apparent changes in macroscopic desensitization after MTS treatment were observed.

$MTSET^+$ and $MTSES^-$ reaction rates

The electrostatic potential near an introduced cysteine can be measured by comparing the second-order reaction rates of a negatively and a positively charged MTS reagent (Karlin and Akabas, 1998). For $\alpha_1\beta_2$K213C and $\alpha_1\beta_2$K215C receptors, $MTSET^+$ rates were 80 and 43 times faster than $MTSES^-$ rates, respectively (Fig. 6, Table 2). In contrast, the rate of $MTSET^+$ modification of the simple thiol 2-mercaptoethanol in solution is only 12.5-fold faster than the rate with $MTSES^-$ (Table 2). To factor out the intrinsic differences in the reactivity of the two reagents, we divided the ratio of the rates of the two reagents at an introduced cysteine by the ratio of the rates for the two reagents with mercaptoethanol (Stauffer and Karlin, 1994; Cheung and Akabas, 1997; Yang et al., 1997). For β_2K213C, the ratio of ratios is $\rho = 80/12.5 = 6.4$ and for β_2K215C, $\rho = 43/12.5 = 3.4$. A ratio of ratios of ~1 indicates that there is no charge selectivity at that

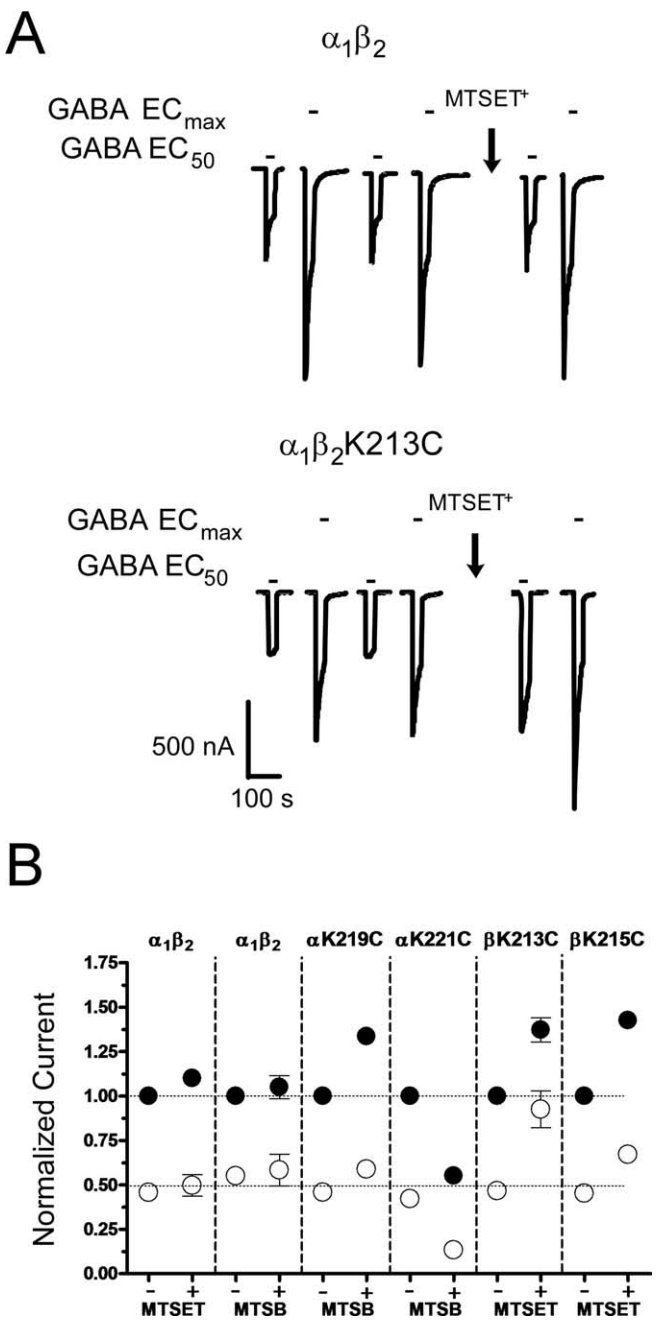

Figure 5. Effects of MTS reagents on GABA maximal currents. ***A***, Representative GABA-mediated current traces from oocytes expressing wild-type ($\alpha_1\beta_2$) and $\alpha_1\beta_2$K213C receptors. Currents elicited by an EC_{50} concentration of GABA and a maximum concentration of GABA (10 mM; EC_{max}) were recorded before and after a 2 min MTS (2 mM) exposure. For $\alpha_1\beta_2$K213C receptors, $MTSET^+$ modification potentiated both GABA EC_{50} and EC_{max} responses. ***B***, Summary of the peak current responses elicited by GABA EC_{max} (filled circles) and GABA EC_{40-60} (open circles) concentrations before (−) and after (+) MTS application for $\alpha_1\beta_2$ and mutant receptors are shown. Data for each receptor were normalized to the peak response to GABA EC_{max} before (−) addition of the MTS reagent and represent the mean ± SEM from at least three independent experiments. $MTSET^+$ and MTSEA-biotin (MTSB) treatment had no effect on $\alpha_1\beta_2$ GABA$_A$ receptor current responses but significantly altered the current responses elicited by GABA EC_{50} and EC_{max} concentrations ($p < 0.01$) for all mutant receptors.

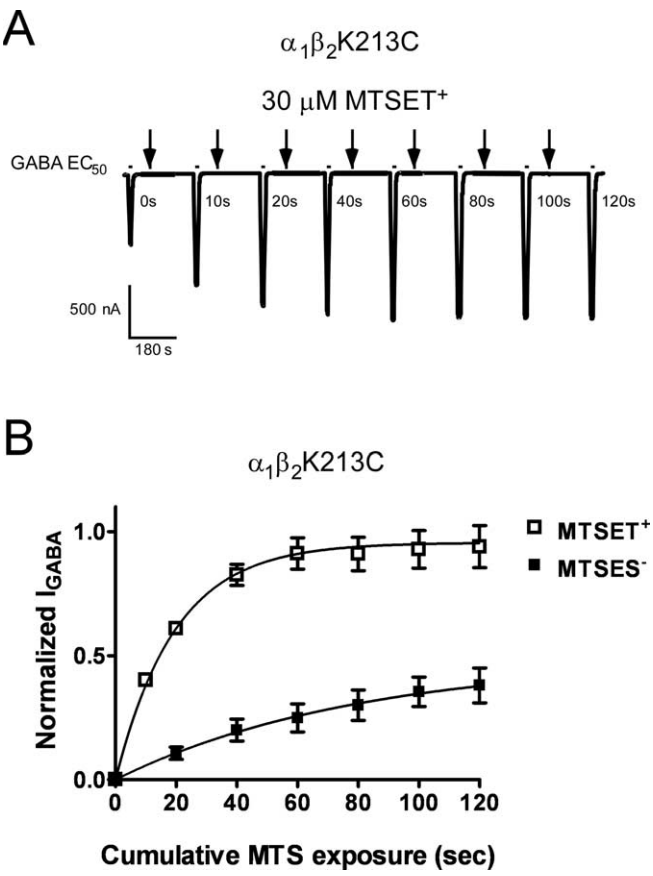

Figure 6. $MTSET^+$ and $MTSES^-$ reaction rates. ***A***, Representative current traces recorded while measuring the rate of $MTSET^+$ modification of $\alpha_1\beta_2$K213C receptors in the absence of GABA. GABA EC_{40-60} current responses were recorded before and after successive application (10–20 s) of 30 μM $MTSET^+$ (arrows). ***B***, Normalized GABA current responses were plotted versus cumulative time of $MTSET^+$ (□) or $MTSES^-$ (500 μM; ■) exposure and fit with single-exponential functions. Data were normalized to the current measured at time = 0 and are (mean ± SEM) from at least four independent experiments. Second-order rate constants (k_2) are reported in Table 2.

position. A ratio of ratios that is significantly larger than one indicates that there is a negative potential experienced by the thiol.

We can estimate the effective electrostatic potential at an introduced cysteine by using the following equation: $\phi = -(1/z_{MTSET} - z_{MTSES})(RT/F)\ln(\rho)$, where z is the unitary charge of the MTS reagent, R is the gas constant, T is absolute temperature, F is Faraday's constant, and ρ is the ratio of ratios calculated above (Stauffer and Karlin, 1994; Yang et al., 1997; Karlin and Akabas, 1998). The calculated negative electrostatic potentials at β_2K213C and β_2K215C in the resting state are −24 and −15 mV, respectively.

Effect of GABA on MTS reaction rates

To determine whether the pre-M1 regions undergoes structural rearrangements during channel gating, we measured the rates of MTS modification of α_1K219C, α_1K221C, β_2K213C, and β_2K215C in the absence ("closed," resting state) and presence of near-saturating GABA (open/desensitized states). The closed reaction rates were all ~2000 $M^{-1}\cdot s^{-1}$ (Fig. 7*D*, Table 3). For $\alpha_1\beta_2$K213C and $\alpha_1\beta_2$K215C receptors, the $MTSET^+$ reaction rates were three and four times faster in the presence of EC_{80-90} GABA, respectively (Fig. 7, Table 3). In contrast, MTSEA-biotin modified α_1K219C approximately three times slower than in its absence, and GABA had no significant effect on the rate of modification of α_1K221C (Fig. 7*C*, Table 3). The alterations in the rates of modifications of α_1K219C, β_2K213C, and β_2K215C in the presence of GABA demonstrate that GABA activation of the

Table 2. Second-order rate constants for $MTSES^-$ and $MTSET^+$ modification of $\alpha_1\beta_2$K213C and $\alpha_1\beta_2$K215C receptors

	$MTSES^-$		$MTSET^+$		
Receptor	k_2 ($M^{-1}\cdot s^{-1}$)	n	k_2 ($M^{-1}\cdot s^{-1}$)	n	$k_2\,ET^+/k_2\,ES^-$
$\alpha_1\beta_2$K213C	23.7 ± 4.3	4	1900 ± 340	5	80 ± 5
$\alpha_1\beta_2$K215C	46.3 ± 9.6	5	1990 ± 220	6	43 ± 1
2-ME[a]	17,000		212,000		12.5

Rates of covalent modification of cysteine mutant receptors were measured as described in Materials and Methods. k_2 values represent the mean ± SEM of second-order rate constants of at least four experiments. ET^+, $MTSET^+$; ES^-, $MTSES^-$.

[a]Reported by Karlin and Akabas (1998) and reflects the rate at which each MTS compound reacts with 2-mercaptoethanol (2-ME) in solution.

receptor triggers movements in or near the pre-M1 regions of both the α_1 and β_2 subunits.

Recently, it has been proposed that β_2D146 (loop 7, Cys–Cys loop) moves closer to β_2K215C (pre-M1) in the open/desensitized state (Kash et al., 2004). If a negatively charged residue is moving closer to the pre-M1 region during receptor activation, then this could explain the increases in the rates of $MTSET^+$ modification of β_2K213C and β_2K215C measured when GABA is present (Fig. 7, Table 3). To test this hypothesis, we examined the ability of $MTSES^-$ (2 mM) to modify β_2K215C in the presence of GABA. We reasoned if GABA activation of the receptor resulted in an increase in the negative electrostatic potential near β_2K215C, then reaction with $MTSES^-$ would be slowed or eliminated in the presence of GABA. Application of $MTSES^-$ alone increased I_{GABA} 47 ± 5% (Fig. 4). Interestingly, when GABA was coapplied with $MTSES^-$, the treatment had no effect. To determine whether $MTSES^-$ reacted silently with β_2K215C, we applied $MTSES^-$ first in the presence of GABA and then in its absence (data not shown). When $MTSES^-$ was subsequently applied in the absence of GABA, GABA currents were potentiated, indicating that $MTSES^-$ does not covalently modify β_2K215 when the receptor is bound with GABA. The data are consistent with the idea that activation of the receptor by GABA induces an increase in the negative electrostatic potential near β_2K215C, which inhibits $MTSES^-$ from reacting with the introduced cysteine.

Discussion

Structural pathway linking agonist binding to channel gating

Structural studies suggest that acetylcholine binding to the nAChR induces a 10° clockwise rotation of the inner β strands of the extracellular ligand binding domain of the α subunit. It is postulated that this rigid body rotation is then translated to the transmembrane M2 channel-lining helix via the β_1–β_2 loop (loop 2) (Miyazawa et al., 2003; Unwin, 2005). Functional studies, using rate–equilibrium free energy relationships, suggest a temporal sequence of events in which agonist binding triggers a conformational wave that begins at the binding site, followed by movements of loops 2 and 7 (Cys–Cys loop) and then the M2–M3 linker, and finally movements of the transmembrane α helices (Grosman et al., 2000a,b; Chakrapani et al., 2004). A recent study using a chimeric receptor comprised of AChBP fused to the transmembrane pore domain of the serotonin type-3A ($5\text{-}HT_{3A}$) receptor showed that only when loops 2, 7, and 9 from AChBP were replaced with $5\text{-}HT_{3A}$ receptor sequence was functional communication between the ligand binding site and channel domain restored, indicating that these loops are critical elements involved in coupling ligand binding to channel gating (Bouzat et al., 2004). It should be noted, however, that the above chimeric receptor contained the charged pre-M1 region of the $5\text{-}HT_{3A}$ receptor, which raises the possibility that the pre-M1 region is also involved in transducing binding to gating.

Here, we provide evidence that the pre-M1 regions of the $GABA_A$ receptor α_1 and β_2 subunits play pivotal roles in coupling binding site movements to the channel domain. The rates of MTS modification of α_1K219C, β_2K213C, and β_2K215C were significantly altered in the presence of GABA (Fig. 7, Table 3), demonstrating that the pre-M1 regions undergo structural rearrangements in response to channel activation, as predicted if the pre-M1 regions propagate structural movements from the binding site to the transmembrane domain. Tethering thiol-reactive groups onto these same residues (α_1K219C, β_2K213C, and β_2K215C) increased maximal GABA-activated currents (Fig. 5), suggesting that structural perturbations of the pre-M1 regions alter channel gating. Finally, cysteine substitution of β_2R216 abolished channel gating by GABA without altering [^{3}H]muscimol binding (Fig. 3), indicating that this residue plays a key role in allosterically coupling GABA binding to gating. Interestingly, the β_2R216C mutation also abolished channel gating by pentobarbital and suggests that this residue may be part of a common activation pathway used by both drugs.

Additional support for a role of the β_2 subunit pre-M1 region in transducing binding site movements to channel gating movements comes from its location. It physically links loop C of the binding site to the membrane domain. Structural studies (Unwin et al., 2002; Celie et al., 2004) as well as molecular dynamic simulations (Henchman et al., 2005) reveal that agonist binding promotes movement of loop C inward to cap the binding site. We predict that this capping movement is propagated to the channel transmembrane domain by the pre-M1 region. In particular, β_2R216 appears to be a key player. This residue is absolutely conserved in every member of the Cys-loop receptor superfamily, and its mutation has been shown to alter agonist-induced channel gating in other Cys-loop receptors (Vicente-Agullo et al., 2001; Hu et al., 2003; Castaldo et al., 2004). A model of the $GABA_A$ receptor shows β_2R216 in close proximity to β_2E52 (Fig. 8), which is also highly conserved, suggesting that these residues electrostatically interact and potentially form a salt bridge linking the pre-M1 region and loop 2. Using this structural pathway, we envision agonist-induced movements in the loop C region of the binding site being propagated to the pre-M1 region, loop 2, and the top of the M2 channel lining helix, which can then bring about channel opening.

Electrostatic network of interactions

The precise details of how the pre-M1 region influences these movements still remain to be worked out. Although the 4 Å structure of the nicotinic acetylcholine receptor provides information about the path of the peptide backbone, residue side-chain position is difficult to determine at this resolution, especially in regions without secondary structure such as those regions that are likely mediating the interactions between the extracellular ligand binding domain (loop 2, loop 7, loop 9, pre-M1) and the transmembrane domain (extracellular end of M1, extracellular end of M2, M2–M3 loop). Here, we demonstrate that the pre-M1 residues αK219C, αK221C, βK213C, and βK215C are located on the water-accessible protein surface, because charged MTS reagents were able to modify these residues (Fig. 4).

Cysteine substitutions of the conserved pre-M1 lysine residues had no effects on GABA EC_{50} (Fig. 2, Table 1), and thus, the positions occupied by the cysteine side chains in the mutant re-

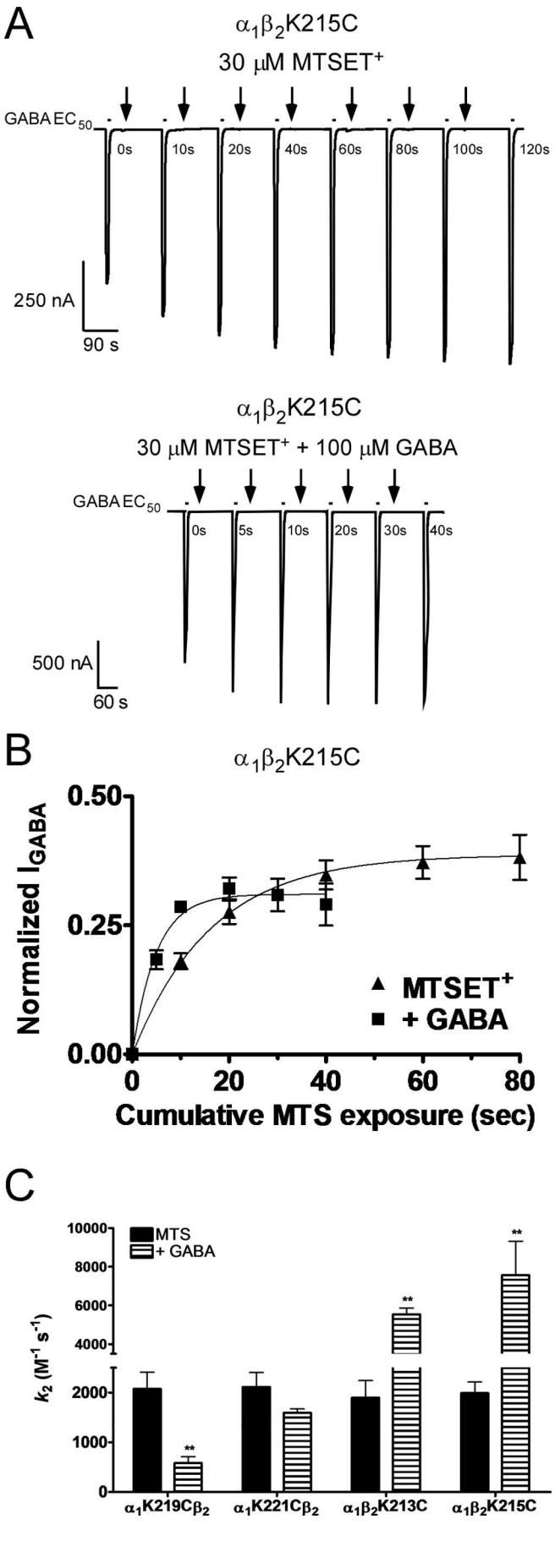

Table 3. Second-order rate constants (k_2) for reaction of MTS reagents with mutant receptors in the absence (control) and presence of GABA

	Control		GABA EC_{80-90}	
Receptor	k_2 ($M^{-1}\cdot s^{-1}$)	n	k_2 ($M^{-1}\cdot s^{-1}$)	n
$\alpha_1K219C\beta_2$[a]	2070 ± 300	4	580 ± 130*	3
$\alpha_1K221C\beta_2$[a]	2110 ± 290	6	1600 ± 80	4
$\alpha_1\beta_2K213C$[b]	1900 ± 340	5	5540 ± 320*	7
$\alpha_1\beta_2K215C$[b]	1990 ± 220	6	7560 ± 1750*	3

Values are mean ± SEM.

[a]MTSEA-biotin reaction rates are reported.

[b]$MTSET^+$ reaction rates are reported.

*$p < 0.001$, significantly different from control.

ceptors are likely similar to the native lysine positions. This allowed us to probe the electrostatic environment of the β_2 pre-M1 region using MTS reagents that differ in charge. $MTSET^+$ modified $\alpha_1\beta_2$K213C and $\alpha_1\beta_2$K215C receptors significantly faster than $MTSES^-$ (Fig. 6, Table 2). In the resting/closed state, we calculated a negative electrostatic potential of −24 mV near β_2K213C and a potential of −15 mV near β_2K215C. A single glutamate residue can contribute approximately −13.5 mV to a local potential (Stauffer and Karlin, 1994). Consistent with this data, in a homology model of the $GABA_A$ receptor, two negatively charged residues β_2D190 (on β-strand 9) and β_2E147 (loop 7) are in close proximity to β_2K213, whereas β_2D146 (loop 7) is near β_2K215 (Fig. 8). The electrostatic potential near the α_1 pre-M1 region could not be measured, because $MTSES^-$ had no functional effect on α_1K219C and $MTSET^+$ had no effect on α_1K221C (Fig. 4). However, the model reveals α_1D148 (loop 7) in close proximity to α_1K219; α_1D54 (loop 2), α_1E143 (loop 7), and α_1D144 (loop 7) near α_1R220; and α_1D191 (on β-strand 9) near α_1K221C (Fig. 9).

Previous studies have suggested that charged residues in loops 2, 7, and the M2–M3 loop play important roles in LGIC activation (Grosman et al., 2000a,b; Absalom et al., 2003; Kash et al., 2003, 2004; Bouzat et al., 2004; Mukhtasimova et al., 2005). It has been reported that an electrostatic interaction between β_2D146 (loop 7) and β_2K215 (pre-M1) is critical for receptor activation based on a double charge swap mutation (β_2D146K, K215D) restoring GABA EC_{50} to near wild-type values compared with single charge reversals (Kash et al., 2004). If gating is controlled by the pair-wise interaction between these residues, one would predict that cysteine mutation of β_2K215, which removes the charge, should alter GABA EC_{50}. This was not observed (Fig. 2, Table 1). Notably, interaction energies obtained from double mutant cycles reflect not only direct pair-wise interactions but can also reflect structural perturbations of neighboring residues as well as interactions between networks of nearby residues (Schreiber and Fersht, 1995), particularly if a residue is coupled

←

Figure 7. Rates of MTS modification of α_1 and β_2 pre-M1 mutant $GABA_A$ receptors in the presence and absence of GABA. ***A***, Rate of sulfhydryl modification of $\alpha_1\beta_2$K215C receptors in the absence and presence of GABA. Representative current traces recorded while applying $MTSET^+$ (30 μM) in the absence (top) and presence (bottom) of GABA (100 μM; EC_{90}). GABA EC_{40-60} current responses were recorded before and after successive applications (10–20 s) of 30 μM $MTSET^+$ alone or coapplied with GABA (arrows). ***B***, Normalized GABA current responses were plotted versus cumulative time of $MTSET^+$ (▲) and $MTSET^+$ coapplied with EC_{80-90} GABA (■) and fit with single-exponential functions. Data were normalized to the current measured at time = 0 and represent mean ± SEM from at least three independent experiments. ***C***, Summary of the second order rate constants (k_2) for reaction of MTS reagents with mutant receptors in the absence (MTS) and presence of GABA (+GABA). Second-order rate constant (k_2) are reported in Table 3. **Values significantly different from MTS alone ($p < 0.001$).

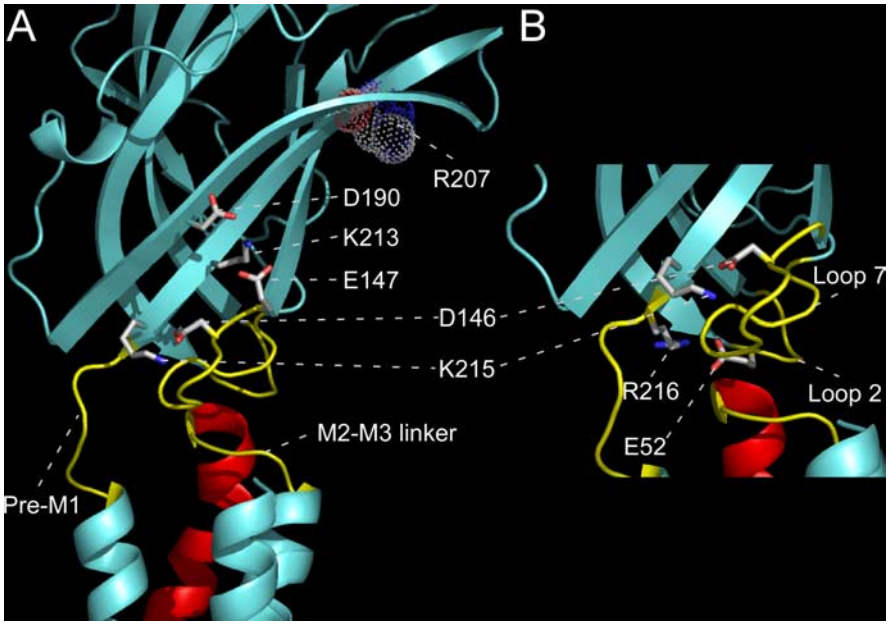

Figure 8. Structural model of the $GABA_A$ receptor β_2 subunit. ***A***, Domains believed to contribute to the transduction mechanism (loop 2, loop 7, M2–M3 linker, and pre-M1) are highlighted in yellow. The pore-forming transmembrane domain 2 (M2) is highlighted in red. Pre-M1 residues β_2K213 and β_2K215 as well as nearby anionic residues are shown in "stick" format. β_2R207, a residue located in the GABA binding site, is shown in a space-filled format. ***B***, Detailed view of the interface between the ligand binding domain and transmembrane domain, which highlights the proximity of residue β_2R216 and β_2E52, which is located in loop 2.

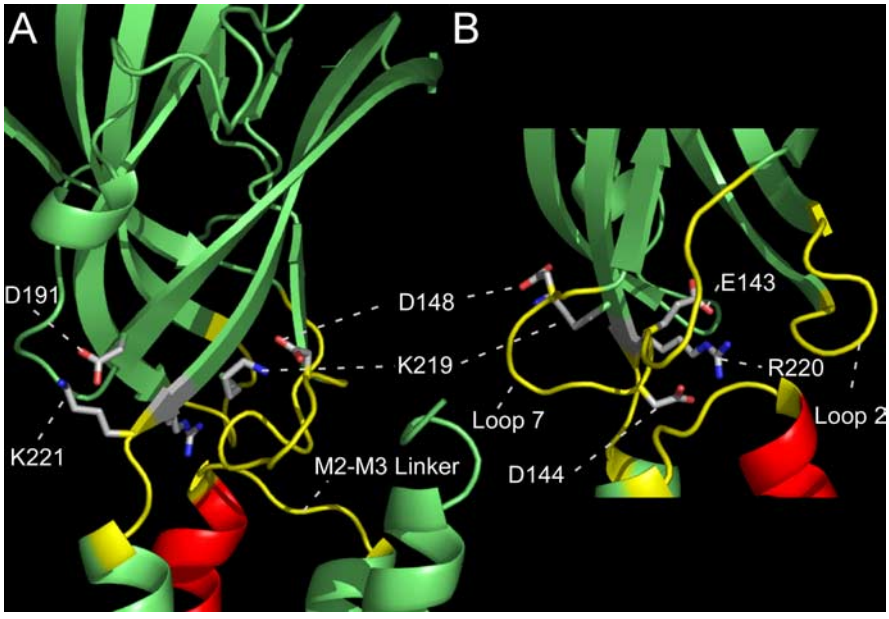

Figure 9. Structural model of the $GABA_A$ receptor α_1 subunit. ***A***, Domains believed to contribute to the transduction mechanism (loop 2, loop 7, M2–M3 linker, and pre-M1) are highlighted in yellow. The pore forming transmembrane domain 2 (M2) is highlighted in red. Pre-M1 residues α_1K221 and α_1K219 as well as nearby anionic residues are shown in "stick" format. ***B***, Detailed view of the interface between the ligand binding domain and transmembrane domain, which highlights two anionic residues (α_1E143 and α_1D144) located in loop 7 nearby the conserved residue α_1R220 at the pre-M1 region.

to others. Our data demonstrating that structurally perturbing the pre-M1 region influences channel gating (Fig. 5) and the finding that significant coupling energies are measured between β_2K215D and a variety of receptor mutations including β_2D139K, β_2D146K, β_2E52K, β_2D56K, and β_2E147K [Kash et al. (2004), their Tables 1, 2] are consistent with β_2K215 and the pre-M1 region being part of a larger network of interacting residues.

Thus, we envision that a network of interactions between residues in the pre-M1 region, loop 2, loop 7, and the top of M2 exists and that coupling of neurotransmitter binding and channel gating (opening, closing, desensitization, and resensitization) is controlled by the forming and breaking of specific sets of contacts between residues in these regions. As a result of the numerous charged residues located in these regions, many of the interactions are likely to be electrostatic. Our data demonstrating that GABA activation of the receptor results in an increase in the negative electrostatic potentials near β_2K215 and β_2K213 (Table 3) as well as previous data in the $GABA_AR$ α_1 subunit demonstrating interactions between charged residues in loop 2, loop 7, and the M2–M3 loop (Kash et al., 2003) are consistent with this idea. The kinetics of salt bridge breaking is estimated to be ~200 ns (Sheldahl and Harvey, 1999; Gruia et al., 2003), and thus, the breaking and forming of salt bridges is potentially a fast enough mechanism for transducing movements from the binding site to the channel domain.

Experiments using rate–equilibrium free energy relationships (Chakrapani et al., 2004) suggest that the transduction of binding to gating occurs as sequential, coupled movements of "rigid body domains," with the ligand binding domain moving first ($\phi \sim 0.9$), loop 2 and loop 7 next ($\phi \sim 0.8$), then the M2–M3 extracellular loop ($\phi \sim 0.7$), and finally the transmembrane domains ($\phi \sim 0.3$–$0.$) Although a ϕ map of the pre-M1 region has not been reported, our data are consistent with the pre-M1 region being part of the loop 2/loop 7 rigid body domain. Although detailed kinetic analyses as well as multiple mutant cycle analysis of mutations are needed to map the specific networks within these rigid body domains as well as between domains, our data demonstrate that the pre-M1 region and in particular β_2R216 are important structural elements involved in coupling neurotransmitter binding to channel gating.

References

Absalom NL, Lewis TM, Kaplan W, Pierce KD, Schofield PR (2003) Role of charged residues in coupling ligand binding and channel activation in the extracellular domain of the glycine receptor. J Biol Chem 278:50151–50157.

Amin J, Weiss DS (1993) GABAA receptor needs two homologous domains of the beta-subunit for activation by GABA but not by pentobarbital. Nature 366:565–569.

Boileau AJ, Czajkowski C (1999) Identification of transduction elements for

benzodiazepine modulation of the $GABA_A$ receptor: three residues are required for allosteric coupling. J Neurosci 19:10213–10220.

Boileau AJ, Kucken AM, Evers AR, Czajkowski C (1998) Molecular dissection of benzodiazepine binding and allosteric coupling using chimeric gamma-aminobutyric acidA receptor subunits. Mol Pharmacol 53:295–303.

Boileau AJ, Evers AR, Davis AF, Czajkowski C (1999) Mapping the agonist binding site of the $GABA_A$ receptor: evidence for a β-strand. J Neurosci 19:4847–4854.

Bouzat C, Gumilar F, Spitzmaul G, Wang HL, Rayes D, Hansen SB, Taylor P, Sine SM (2004) Coupling of agonist binding to channel gating in an ACh-binding protein linked to an ion channel. Nature 430:896–900.

Brejc K, van Dijk WJ, Klaassen RV, Schuurmans M, van Der Oost J, Smit AB, Sixma TK (2001) Crystal structure of an ACh-binding protein reveals the ligand-binding domain of nicotinic receptors. Nature 411:269–276.

Castaldo P, Stefanoni P, Miceli F, Coppola G, Miraglia Del Giudice E, Bellini G, Pascotto A, Trudell JR, Harrison NL, Annunziato L, Taglialatela M (2004) A novel hyperekplexia-causing mutation in the pre-transmembrane segment 1 of the human glycine receptor alpha 1 subunit reduces membrane expression and impairs gating by agonists. J Biol Chem 279:25598–25606.

Celie PH, van Rossum-Fikkert SE, van Dijk WJ, Brejc K, Smit AB, Sixma TK (2004) Nicotine and carbamylcholine binding to nicotinic acetylcholine receptors as studied in AChBP crystal structures. Neuron 41:907–914.

Chakrapani S, Bailey TD, Auerbach A (2004) Gating dynamics of the acetylcholine receptor extracellular domain. J Gen Physiol 123:341–356.

Cheung M, Akabas MH (1997) Locating the anion-selectivity filter of the cystic fibrosis transmembrane conductance regulator (CFTR) chloride channel. J Gen Physiol 109:289–299.

Cromer BA, Morton CJ, Parker MW (2002) Anxiety over GABA(A) receptor structure relieved by AChBP. Trends Biochem Sci 27:280–287.

Dennis M, Giraudat J, Kotzyba-Hibert F, Goeldner M, Hirth C, Chang JY, Lazure C, Chretien M, Changeux JP (1988) Amino acids of the *Torpedo marmorata* acetylcholine receptor alpha subunit labeled by a photoaffinity ligand for the acetylcholine binding site. Biochemistry 27:2346–2357.

Galzi JL, Revah F, Bouet F, Menez A, Goeldner M, Hirth C, Changeux JP (1991a) Allosteric transitions of the acetylcholine receptor probed at the amino acid level with a photolabile cholinergic ligand. Proc Natl Acad Sci USA 88:5051–5055.

Galzi JL, Bertrand D, Devillers-Thiery A, Revah F, Bertrand S, Changeux JP (1991b) Functional significance of aromatic amino acids from three peptide loops of the alpha 7 neuronal nicotinic receptor site investigated by site-directed mutagenesis. FEBS Lett 294:198–202.

Grosman C, Zhou M, Auerbach A (2000a) Mapping the conformational wave of acetylcholine receptor channel gating. Nature 403:773–776.

Grosman C, Salamone FN, Sine SM, Auerbach A (2000b) The extracellular linker of muscle acetylcholine receptor channels is a gating control element. J Gen Physiol 116:327–340.

Gruia AD, Fischer S, Smith JC (2003) Molecular dynamics simulation reveals a surface salt bridge forming a kinetic trap in unfolding of truncated Staphylococcal nuclease. Proteins 50:507–515.

Henchman RH, Wang HL, Sine SM, Taylor P, McCammon JA (2005) Ligand-induced conformational change in the alpha7 nicotinic receptor ligand binding domain. Biophys J 88:2564–2576.

Holden JH, Czajkowski C (2002) Different residues in the GABA(A) receptor alpha 1T60-alpha 1K70 region mediate GABA and SR-95531 actions. J Biol Chem 277:18785–18792.

Hu XQ, Zhang L, Stewart RR, Weight FF (2003) Arginine 222 in the pre-transmembrane domain 1 of 5-HT3A receptors links agonist binding to channel gating. J Biol Chem 278:46583–46589.

Kao PN, Dwork AJ, Kaldany RR, Silver ML, Wideman J, Stein S, Karlin A (1984) Identification of the alpha subunit half-cystine specifically labeled by an affinity reagent for the acetylcholine receptor binding site. J Biol Chem 259:11662–11665.

Karlin A, Akabas MH (1998) Substituted-cysteine accessibility method. Methods Enzymol 293:123–145.

Kash TL, Jenkins A, Kelley JC, Trudell JR, Harrison NL (2003) Coupling of agonist binding to channel gating in the GABA(A) receptor. Nature 421:272–275.

Kash TL, Dizon MJ, Trudell JR, Harrison NL (2004) Charged residues in the beta2 subunit involved in GABAA receptor activation. J Biol Chem 279:4887–4893.

Laskowski RA, Rullmannn JA, MacArthur MW, Kaptein R, Thornton JM (1996) AQUA and PROCHECK-NMR: programs for checking the quality of protein structures solved by NMR. J Biomol NMR 8:477–486.

Liman ER, Tytgat J, Hess P (1992) Subunit stoichiometry of a mammalian K^+ channel determined by construction of multimeric cDNAs. Neuron 9:861–871.

Mishina M, Tobimatsu T, Imoto K, Tanaka K, Fujita Y, Fukuda K, Kurasaki M, Takahashi H, Morimoto Y, Hirose T, Inayama S, Takahashi T, Kuno M, Numa S (1985) Location of functional regions of acetylcholine receptor alpha-subunit by site-directed mutagenesis. Nature 313:364–369.

Miyazawa A, Fujiyoshi Y, Unwin N (2003) Structure and gating mechanism of the acetylcholine receptor pore. Nature 424:949–955.

Mukhtasimova N, Free C, Sine SM (2005) Initial coupling of binding to gating mediated by conserved residues in the muscle nicotinic receptor. J Gen Physiol 126:23–39.

Pascual JM, Karlin A (1998) State-dependent accessibility and electrostatic potential in the channel of the acetylcholine receptor. Inferences from rates of reaction of thiosulfonates with substituted cysteines in the M2 segment of the alpha subunit. J Gen Physiol 111:717–739.

Powell JMD (1977) Restart procedures for the conjugate gradient method. Math Program 12:241–251.

Press WH, Flannery BP, Teukolsky SA, Vetterling WT (1988) Numerical recipes in C: the art of scientific computing. In: Minimization and maximization of functions, Ed 1, Chap 10, pp 301–327. Cambridge, UK: Cambridge UP.

Rajendra S, Vandenberg RJ, Pierce KD, Cunningham AM, French PW, Barry PH, Schofield PR (1995) The unique extracellular disulfide loop of the glycine receptor is a principal ligand binding element. EMBO J 14:2987–2998.

Robertson GA, Warmke JM, Ganetzky B (1996) Potassium currents expressed from *Drosophila* and mouse eag cDNAs in *Xenopus* oocytes. Neuropharmacology 35:841–850.

Ruiz-Gomez A, Morato E, Garcia-Calvo M, Valdivieso F, Mayor Jr F (1990) Localization of the strychnine binding site on the 48-kilodalton subunit of the glycine receptor. Biochemistry 29:7033–7040.

Schreiber G, Fersht AR (1995) Energetics of protein-protein interactions: analysis of the barnase-barstar interface by single mutations and double mutant cycles. J Mol Biol 248:478–486.

Sheldahl C, Harvey SC (1999) Molecular dynamics on a model for nascent high-density lipoprotein: role of salt bridges. Biophys J 76:1190–1198.

Stauffer DA, Karlin A (1994) Electrostatic potential of the acetylcholine binding sites in the nicotinic receptor probed by reactions of binding-site cysteines with charged methanethiosulfonates. Biochemistry 33:6840–6849.

Unwin N (2005) Refined structure of the nicotinic acetylcholine receptor at 4A resolution. J Mol Biol 346:967–989.

Unwin N, Miyazawa A, Li J, Fujiyoshi Y (2002) Activation of the nicotinic acetylcholine receptor involves a switch in conformation of the alpha subunits. J Mol Biol 319:1165–1176.

Vandenberg RJ, French CR, Barry PH, Shine J, Schofield PR (1992a) Antagonism of ligand-gated ion channel receptors: two domains of the glycine receptor alpha subunit form the strychnine-binding site. Proc Natl Acad Sci USA 89:1765–1769.

Vandenberg RJ, Handford CA, Schofield PR (1992b) Distinct agonist- and antagonist-binding sites on the glycine receptor. Neuron 9:491–496.

Vicente-Agullo F, Rovira JC, Sala S, Sala F, Rodriguez-Ferrer C, Campos-Caro A, Criado M, Ballesta JJ (2001) Multiple roles of the conserved key residue arginine 209 in neuronal nicotinic receptors. Biochemistry 40:8300–8306.

Wagner DA, Czajkowski C (2001) Structure and dynamics of the GABA binding pocket: a narrowing cleft that constricts during activation. J Neurosci 21:67–74.

Yang N, George Jr AL, Horn R (1997) Probing the outer vestibule of a sodium channel voltage sensor. Biophys J 73:2260–2268.